Heliyon 10 (2024) e25454

Contents lists available at ScienceDirect

Heliyon

journal homepage: www.cell.com/heliyon

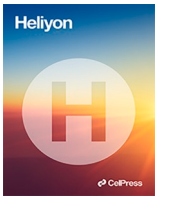

Research article

Silver nanoparticles biogenically synthesised using *Maclurodendron porteri* extract and their bioactivities

Nadhirah Badrillah [a], Deny Susanti [b,c,**], Tengku Karmila Tengku Mohd Kamil [d], Greesty Finotory Swandiny [c,***], Yuli Widyastuti [e], Erizal Zaini [f,****], Muhammad Taher [a,c,g,*]

[a] *Department of Pharmaceutical Technology, Faculty of Pharmacy, International Islamic University Malaysia, Jalan Sultan Ahmad Shah, 25200, Kuantan, Pahang, Malaysia*
[b] *Department of Chemistry, Faculty of Science, International Islamic University Malaysia, Jalan Sultan Ahmad Shah, 25200, Kuantan, Pahang, Malaysia*
[c] *Faculty of Pharmacy, Pancasila University, Srengseng Sawah, 12630, Jakarta, Indonesia*
[d] *Department of Pharmacy Practice, Faculty of Pharmacy, International Islamic University Malaysia, Jalan Sultan Ahmad Shah, 25200, Kuantan, Pahang, Malaysia*
[e] *Research Centre for Pharmaceutical Ingredients and Traditional Medicine, National Research and Innovation Agency, Jl. Raya Lawu 11, 10 Tawangmangu, Karanganyar, Central Java, 57792, Indonesia*
[f] *Faculty of Pharmacy, Universitas Andalas, 25175, Padang, Indonesia*
[g] *Pharmaceutics and Translational Research Group, Kulliyyah of Pharmacy, International Islamic University Malaysia, 25200, Kuantan, Pahang, Malaysia*

ARTICLE INFO

Keywords:
Silver nanoparticles
Green synthesis
Maclurodendron porteri
Antibacterial activity
Cytotoxic activity

ABSTRACT

Silver nanoparticle is widely used in various field including medical, cosmetic, food and industrial purposes due to their unique properties in electrical conductivity, thermal, and biological activities. In the medical field, silver nanoparticles (AgNPs) have been reported to have strong antimicrobial and cytotoxic activities. This study aimed to synthesize and characterize silver nanoparticles (AgNPs) using *Maclurodendron porteri* (MP) extract and to evaluate the antimicrobial and cytotoxic activities of the synthesised MP-AgNPs. Green method of Ultrasound Assisted Extraction (UAE) was used to extract the leaves of *M. porter*. Liquid Chromatography -Mass Spectrometry/Quadrupole time-of-flight (LC-MS/QTOF) was used to identify the compounds in the leaf extract *of M. porteri*. Characterisation of the synthesised nanoparticles involved ultraviolet–visible (UV–Vis), Fourier Transform Infrared (FTIR), scanning electromagnetic microscopy (SEM), Zeta potential Analyzer and Particle Size Analyzer. The cytotoxic assay was conducted on MCF-7 and Caco-2 cell lines by MTT assay. Antimicrobial activity was tested on Gram-negative and Gram-positive bacteria using the disc diffusion method. Based on LC-MS/QTOF analysis, 430 compounds were found. The identified major compounds consist of amino acids, polyphenols, steroids, terpenoids and heterocyclic compounds which possibly act as reducing agents. 1 mM, 5 mM and 10 mM of silver nitrate solution were mixed with the leaf extract to form silver

* Corresponding author. Faculty of Pharmacy, Pancasila University, Srengseng Sawah, 12630, Jakarta, Indonesia.
** Corresponding author. Faculty of Pharmacy, Pancasila University, Srengseng Sawah, 12630, Jakarta, Indonesia.
*** Corresponding author. Faculty of Pharmacy, Pancasila University, Srengseng Sawah, 12630, Jakarta, Indonesia.
**** Corresponding author. Faculty of Pharmacy, Universitas Andalas, 25175, Padang, Indonesia.
E-mail addresses: deny@iium.edu.my (D. Susanti), greestyfinotory@univpancasila.ac.id (G.F. Swandiny), erizal@ffarmasi.unand.ac.id (E. Zaini), mtaher@iium.edu.my (M. Taher).

https://doi.org/10.1016/j.heliyon.2024.e25454
Received 1 September 2023; Received in revised form 26 January 2024; Accepted 26 January 2024
Available online 12 February 2024

nanoparticles. 1.2 mg/ml of MP-AgNPs were found to have antibacterial activity against *B. subtilis, S. aureus, E. coli,* and *P. aeruginosa* with inhibitory zones of 8.0 ± 0.36 mm, 8.5 ± 0.45 mm, 7.5 ± 0.36 mm, and 9.0 ± 0.40 mm respectively. MP-AgNPs showed no cytotoxic activity against Caco-2 and MCF-7 cells. In conclusion, the presence of major amine compounds such as 10,11-dihydro-10,11-dihydroxyprotriptyline and harderoporphyrin in the extract facilitated the synthesis of AgNPs and the nanoparticle showed weak bioactivities in the assay conducted.

1. Introduction

Multiple drug resistance (MDR) is on the rise because of the improper and excessive use of broad-spectrum antibiotics. If no proper initiatives are introduced to combat MDR, it is estimated that by 2050, MDR is accountable for 10 million fatalities every year [1]. Chemoresistance has also been one of the issues as it contributes to the poor prognosis of cancer patients. Patients who have a good response to a certain chemotherapy drug may develop resistance to it in a short time [2]. Therefore, it is necessary to establish cost-effective methods for the synthesis of therapeutic agents that can overcome the problems mentioned above. Nowadays, metallic nanoparticles (NPs) are frequently studied due to their numerous uses in biotechnology and have been proven effective for combating microbial and chemotherapy resistance [3,4].

In general, NPs are structures with sizes ranging from 1 to 100 nm in diameter [5]. Silver, gold, titanium, selenium, iron, copper, and zinc oxide are some known NPs that have all shown high antibacterial activity [6,7]. Silver nanoparticles (AgNPs) have received more attention than other NPs because they exhibit a unique and flexible surface plasmon resonance [8]. Besides, AgNPs possess antibacterial properties that can kill bacteria with several mechanisms including nano perforation, cellular membrane rupture, production of reactive oxygen species (ROS), and disruption of DNA replication [9]. Previous research has also demonstrated that AgNPs have anti-proliferative and apoptosis-inducing characteristics which are hazardous to cancerous cells as they cause DNA damage, oxidative stress, and mitochondrial damage. The bioactivity of AgNPs is influenced by numerous factors, such as size and shape, surface chemistry, size distribution, capping or stabilising agents and agglomeration [10].

AgNPs can be synthesised by physical, chemical, or biological methods. The synthesis of NPs using biological methods is the most economical and environmentally friendly since it consumes natural products from microbes or plant extracts as reducing agents to produce NPs [11]. It involves simple techniques by extracting natural compounds from microorganisms or plants [12]. In comparison to using microorganisms, plant extract-based nanoparticles have the significant benefits of not requiring complicated techniques, having simpler and faster procedures, being cheaper, and easier to scale up for large-scale nanoparticle synthesis [7].

Green synthesis of silver nanoparticles refers to the method that uses water-based extract eco-friendly materials and biocompatible nanoparticle products. Among the green methods for synthesising silver nanoparticles is using plant extract where the plant-based synthesis does not require capping or stabilising agent [13]. Plants contain various active compounds that might important role in the reduction process due to unique functional groups [14]. Terpenoids, glycosides, carbohydrates and vitamin has the capability in reduction, surface coating/capping and stabilisation [15], phenolic compounds such as tannins, flavonoids and phenolic acid have a role in bioreduction as well as act as capping and stabilising agent [14]. Proteins and amino acids are strongly bound to metal nanoparticles, capping and protecting them from agglomeration [16]; therefore alkaloids are known to have a powerful reducing agent [17].

Leaves extract of *Maclurodendron porteri* was used in this study for the green synthesis of AgNPs. *M. porteri* is categorised under *Rutaceae* family and it is also referred as *Merlimau* by the locals [18]. The leaves from the plant contain a variety of phytochemicals and secondary metabolites that can function as reducing, capping, and stabilising agents during the synthesis of NPs [11]. In 1998, two furanoquinoline alkaloids which are skimmianine and kokusaginin were isolated from the leaves of *M. porteri* by Bowen and Osborne. A furanoquinoline alkaloid called haplophytin B was isolated from *M. porteri* [18]. Haplophytin B demonstrated weak antioxidant activity [19], while haplophytin A exhibited apoptosis-inducing effects on HL-60 cells [20].

There is not much research that has been reported related to *M. porteri*. In addition, there was no report of *M. porteri* being used in the biosynthesis of AgNPs. Hence, the present study aimed to synthesize and characterize AgNPs of *M. porteri* by using the green synthesis method and to evaluate the antimicrobial on Gram-positive and Gram-negative bacteria. Cytotoxic activity of MP-AgNPs targeting the most common cancer disease in Malaysia i.e. breast and colon cancer using MCF-7 and Caco-2 cell lines, respectively.

2. Materials and methods

2.1. Plant material and extraction

Leaves of *M. porteri* (Hook. F) T.G. Hartley, voucher specimen (MT-11-07), were collected from IIUM Forest of 'Ilm. The leaves were dried for 3 days and finely ground using a mechanical grinder [21]. The grounded leaves (50 g) were mixed with 500 ml of ethanol (Ethanol 95%, HmbG Chemicals) and distilled water mixture with a ratio of 80:20 v/v [22]. The grounded leaves were extracted in the ethanol/distilled water mixture with Ultrasound-Assisted Extraction (UAE) using a probe sonicator (Qsonica Ultrasonic Sonicator Converter Model CL-334) for 40 min at a temperature of 48 °C. The ultrasound from the probe sonicator promotes swelling, hydration and expansion of the cell wall's pores which enhances the release of compounds from the leaves [23]. A funnel topped with NICE Qualitative 102 filter paper was used to filter the aqueous extract. The filtrate was stored in the refrigerator at 4 °C [24].

2.2. Liquid chromatography-mass spectrometry time of flight (LC-MS/QTOF)

Gummy texture of *M. porteri*'s ethanolic extract (10 mg) was obtained from the drying process using a rotary evaporator. 1 mL of methanol was used to dilute the gummy extract to a final concentration of 10 mg/mL. Then, the extract was diluted again with methanol to a concentration of 1 mg/mL. The extract was filtered with a 0.22 μm pore size syringe filter before performing the analysis using LC-MS/QTOF (model 6520 Agilent Technologies, SA, USA). 2 μl of the filtered extract was injected into Agilent ZORBAX Eclipse Plus C18 Rapid Resolution HT column (2.1 mm × 100 mm × 1.8 μm, Agilent Technologies, SA, USA) at the temperature of 40 °C. The flow rate used was 0.25 mL/min with solvent A (0.1% formic acid in distilled water) and solvent B (0.1% formic acid in acetonitrile). The gradient elution program was 0.00–18.00 min for 5–95% of mobile phase (B), 18–23 min for 95% of mobile phase (B) and 23.01 min for 5% of mobile phase (B). The total run time for analysis of the extract was 30 min. The mass spectrometer was set to positive electrospray ionisation (ESI) mode with an optimal gas temperature of 325 °C, gas flow of 11 L/min, and nebulizer pressure of 35 psi. The Agilent Mass Hunter Qualitative Analysis B.05.00 software (Agilent Technologies, Santa Clara, CA, USA) was used to analyze the MS data and METLIN database was used to annotate the predicted chemical compounds [25].

2.3. Green synthesis of silver nanoparticles (AgNPs)

To make a silver nitrate ($AgNO_3$) solution, $AgNO_3$ powder which was purchased from Emsure (Macedonia) was weighed and dissolved in deionised water. 90 ml of 1 mM, 5 mM and 10 mM of $AgNO_3$ solution was poured into three different beakers covered with aluminium foil to avoid photo-oxidation. Then, 10 mL of *M. porteri* ethanolic extract was added into each of the beakers and stirred continuously for 24 h at room temperature. The change in the colour of the solution indicated the formation of AgNPs [21]. The solution was centrifuged at 10,000 rpm for 15 min at 4 °C by High-Speed Centrifuge Supra 22K (Hanil Science Industrial, Incheon, South Korea) to obtain AgNPs [26]. The resulting pellet was rinsed with deionised water and dried in the oven at 40 °C.

2.4. Silver nanoparticles characterisation

2.4.1. UV–visible (UV–Vis) spectroscopy

During the stirring process, a 1 mL sample of the MP-AgNPs solution was taken at the interval of 1, 2, 6, 8 and 24 h. UV–Visible spectrophotometer (UV–visible 1800, Shimadzu) was used to measure UV–Vis absorption spectra of the samples in the scanning range of 350–800 nm and deionised water was used as the blank.

2.4.2. Fourier transform infra-red (FTIR) spectroscopy

PerkinElmer's Spectrum Two FTIR spectrometer (PerkinElmer Inc, USA) was used to identify the functional group of biosynthesised MP-AgNPs. The sample were placed on a potassium bromide pellet and scanned in the wavelength range from 4000 cm^{-1} to 400 cm^{-1} [22].

2.4.3. Scanning Electron Microscopy (SEM)

The MP-AgNPs solution was dried into a powder, put on a sample holder, and covered with a conductive metal [23]. By using SEM at 20–25 voltage, the morphology and structural characteristics of the synthesised MP-AgNPs were analyzed [8].

2.4.4. Particle size analyzer

1 mL of MP-AgNPs solution was put inside the cuvette and the particle size distribution of MP-AgNPs was analyzed by using Malvern Zetasizer Nano ZS (Malvern Instruments, Worcestershire, UK).

2.4.5. Zeta potential analyzer

Zeta potential analysis was performed using Malvern Zetasizer ZEN 1600 (Malvern Instruments, Worcestershire, UK) to determine the stability and surface charge of colloidal nanoparticles [23]. MP-AgNPs solution (1 mL) was inserted into the capillary of Malvern Panalytical DTS1070 folded capillary zeta cell and the zeta potential was analyzed.

2.5. Antibacterial activity

The disc diffusion method was used to evaluate the antibacterial activity of the synthesised MP-AgNPs against two Gram-positive bacteria (*Bacillus subtilis* ATCC 29970, *Staphylococcus aureus* ATCC 25923) and two Gram-negative bacteria (*Escherichia coli* ATCC 25922, *Pseudomonas aeruginosa* ATCC 10145). Nutrient agar powder (20 g) was dissolved in 1000 mL of distilled water. The mixture was sterilised in an autoclave at 121 °C for 15 min. Each Petri plate was poured with 25 mL of the nutrient agar media and the media was allowed to harden at room temperature. With a cotton swab, the bacterial strains with a concentration of 1.5×10^8 CFU/mL were cultured on the surface of the agar. Blank discs were loaded with 10 μL of MP-AgNPs, *M. porteri* extract and $AgNO_3$ and then impregnated on the agar. Deionised water was the negative control for this antimicrobial study while amoxicillin and streptomycin were chosen as the positive controls. The plates were incubated at 37 °C for 24 h and the clear zone of inhibitions were measured [5].

2.6. Cytotoxic activity

MTT assay was employed to evaluate the cytotoxic activity of MP-AgNPs and *M. porteri* extract. Caco-2 cells (human colorectal adenocarcinoma cells) and MCF-7 cells (human breast cancer cells) were seeded for the assay. Both cells were cultured in a 75 cm^3 tissue culture flasks in Dulbecco's Modified Eagle Medium (DMEM) supplemented with 10% (v/v) Fetal Bovine Serum (FBS) and 1% (v/v) of Penicillin-Streptomycin mixed solution at 37 °C in 5% CO_2 incubator [3,27]. Once the cell confluency reached 80%, trypsinization was performed to detach the cells from the flasks. Caco-2 cells and MCF-7 cells were seeded at a density of 1.0×10^4 per well and 1.5×10^4 per well respectively in 96-well plates. After the treatment, the purple colour of formazan salts formed in the wells treated with MP-AgNPs which indicated the viability of cells [28].

The cells in the 96-well plates were treated with varying concentrations of MP-AgNPs and *M. porteri* extract (400 μg/ml, 200 μg/ml, 100 μg/ml, 50 μg/ml, 25 μg/ml and 12.5 μg/ml) for 24 h at 37 °C in 95% air with 100% humidity and 5% CO_2. Tamoxifen was used as the positive control [29]. Then, the cells were treated with 100 μl of 5 mg/ml 3-[4,5-dimethylthiazol-2-yl]-2,5-diphenyltetrazolium bromide (MTT) at 37 °C for 4 h 100 μL of dimethyl sulfoxide (DMSO) was used to dissolve the synthesised formazan salt crystals, which indicated the vitality of the cells, and then incubated at 37 °C for an additional 30 min [3]. Using a microplate reader (Infinite M200 Nanoquant, Tecan Austria), the absorbance were recorded at 570 nm. Equation (1) was used to calculate the percentage of cell viability [27]:

$$\text{Cell viability } (\%) = \frac{A\ sample}{A\ untreated} \text{ x } 100 \tag{1}$$

A sample is the absorbance of cells treated with the samples; MP-AgNs and *M. porteri* extract. Meanwhile, untreated is the absorbance of the cells that are not treated with the samples.

2.7. Statistical analysis

Statistical analysis was performed by using SPSS (Statistical Package for Social Sciences). Tests were conducted in triplicates. The resulting data from the tests were presented as mean ± standard error (SE) by using One-Way ANOVA while Duncan's technique was used to find individual correlations. A difference was determined to be significant at $p < 0.05$ [5].

3. Results and discussions

3.1. LC-MS/QTOF based profiling of M. porteri extract

M. porteri extract was analyzed by utilising data analysis software (Agilent Mass Hunter Qualitative Analysis B.05.00 software). Using METLIN database, the accurate masses of compounds with predicted chemical formulas were identified [25]. 430 compounds were found by the LC-MS/QTOF profile of *M. porteri* extract with a retention time of 30 min (Fig. 1). 10,11-Dihydro-10,11-dihydroxyprotriptyline, harderoporphyrin, ethylketocyclazocine, pheophorbide a, eplerenone, D-Proline, and tangeraxanthin are the major compounds identified in the leaves of *M. porteri* extract (Table 1). However, few other major compounds were unknown as the molecular formula and accurate masses of the compounds were unavailable in the database.

Based on the literature, the plant metabolites such as amine, amino acids, polyphenols, steroids, terpenoids and heterocyclic compounds are capable of capping, stabilising and bioreduction of metal nanoparticles [10,30]. Since the major compounds listed in Table 1 like 10,11-Dihydro-10,11-dihydroxyprotriptyline, harderoporphyrin, ethylketocyclazocine and pheophorbide a contain carboxyl, hydroxyl and amine groups that reported to act as reducing agent [8], thus the compounds may be possible to involve in the synthesis of AgNPs.

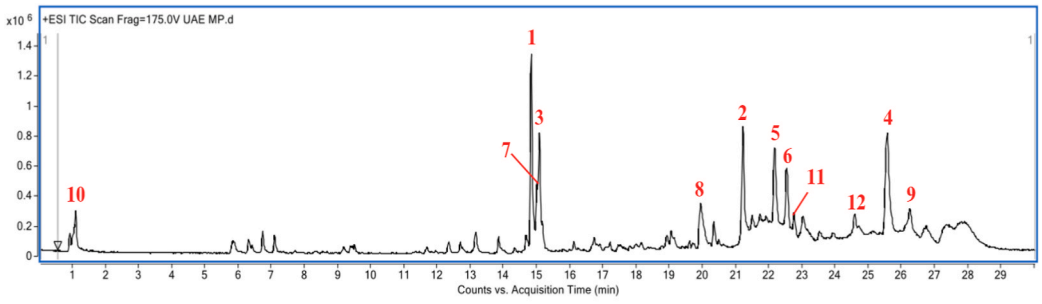

Fig. 1. LC-MS Chromatogram of *M. porteri* extract. LC was run on a Agilent ZORBAX Eclipse Plus C18 Rapid Resolution HT column (2.1 mm × 100 mm × 1.8 μm, Agilent Technologies, SA, USA) at the temperature of 40 °C. The flow rate used was 0.25 mL/min with solvent A (0.1% formic acid in distilled water) and solvent B (0.1% formic acid in acetonitrile). The mass spectrometer was set to positive electrospray ionisation (ESI) mode with an optimal gas temperature of 325 °C, gas flow of 11 L/min, and nebulizer pressure of 35 psi.

Table 1
Predicted major compounds of *M. porteri* extract.

No	Name of compound	Formula	Mass
1.	10,11-Dihydro-10,11-dihydroxyprotriptyline	$C_{19}H_{23}NO_2$	297.1728
2.	Harderoporphyrin	$C_{35}H_{36}N_4O_6$	608.2632
3.	Ethylketocyclazocine	$C_{19}H_{25}NO_2$	299.1888
4.	Unknown compound	–	620.2998
5.	Pheophorbide a	$C_{35}H_{36}N_4O_5$	592.2686
6.	Unknown compound	–	533.2778
7.	Eplerenone	$C_{24}H_{30}O_6$	414.2041
8.	Unknown compound	–	465.2147
9.	Unknown compound	–	620.2993
10.	D-Proline	$C_5H_9NO_2$	115.0634
11.	Tangeraxanthin	$C_{34}H_{44}O_2$	484.3338
12.	Unknown compound	–	606.2835

3.2. Production of MP-AgNPs by green synthesis

As 10 mL of *M. porteri* extract was mixed with 90 mL of $AgNO_3$ solution with different concentrations (1 mM, 5 mM and 10 mM), the weight of yield was observed and recorded (Fig. 2). The different concentrations of $AgNO_3$ solution were directly proportional to the yield of MP-AgNPs. A higher (10 mM) concentration of $AgNO_3$ solution resulted in a higher yield. 10 mM of $AgNO_3$ solution had the highest yield of MP-AgNPs with an amount of only 121 mg, followed by 5 mM and 1 mM of $AgNO_3$ solution with the yield amount of 86 g and 10 g respectively.

The amino acids, polyphenols, steroids, terpenoids and heterocyclic compounds in the *M. porteri* extract might be responsible for acting as a reducing agent as they mediated the reduction and stabilisation of MP-AgNPs. The process involved the oxidation of polysaccharide hydroxyl groups to carboxyl groups. The liberated reactive hydrogen worked as a reducing agent by binding to the $AgNO_3$ and converted Ag^+ into Ag^0 to produce AgNPs [8,30]. Equation (2) is the proposed mechanism of reduction reaction for green synthesis of MP-AgNPs [28].

$$Ag^+ NO_3^- + \text{Phytochemicals of } \textit{M. porteri} \text{ extract (-C═O, –OH, –NH, etc.)} \longrightarrow Ag^0 \text{ NPs } \ldots\ldots \quad (2)$$

3.3. Characterisation of MP-AgNPs

3.3.1. Visual observation of MP-AgNPs formation

The colour change of the *M. porteri* extract and $AgNO_3$ solution mixture can be observed from light yellow to a slightly darker colour after 24 h of mixing (Fig. 3). The change of colour indicated MP-AgNPs formation and the phenomenon happened due to the excitation of the surface plasmon resonance during the green synthesis of AgNPs [23].

3.3.2. UV–vis analysis

The formation of synthesised MP-AgNPs was further proven by UV–visible spectroscopy. As the mixing duration of the samples increased, the absorbance values were also increased. The sample with 24-h mixing duration showed the peak with the highest absorbance value compared to 1, 2, 6 and 8-h mixing duration, suggesting the highest amount of MP-AgNPs formation was at 24 h. The highest absorption peak was observed at 455 nm (Fig. 4). The presence of peaks at a spectrum ranging from 400 to 490 nm suggested the presence of AgNPs due to the excitation of the surface plasmons [23,31]. The broadness of the band reflected the physical

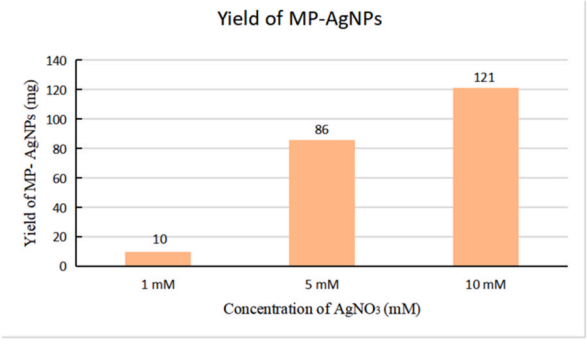

Fig. 2. Yield of MP-AgNPs with different concentrations of $AgNO_3$ solution. Different concentration of $AgNO_3$ (1, 5 or 10 mM) was added to undergo the biogenic synthesis with the extract.

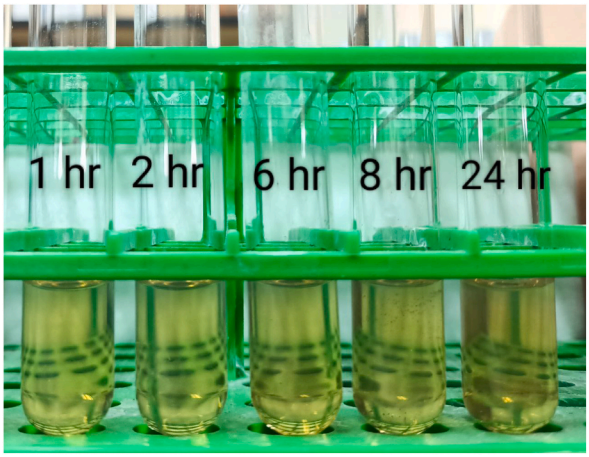

Fig. 3. Visual observation of MP-AgNPs formation. The reaction was observed at 1,2,6,8 and 24 h. The amount of synthesised AgNPs was monitored.

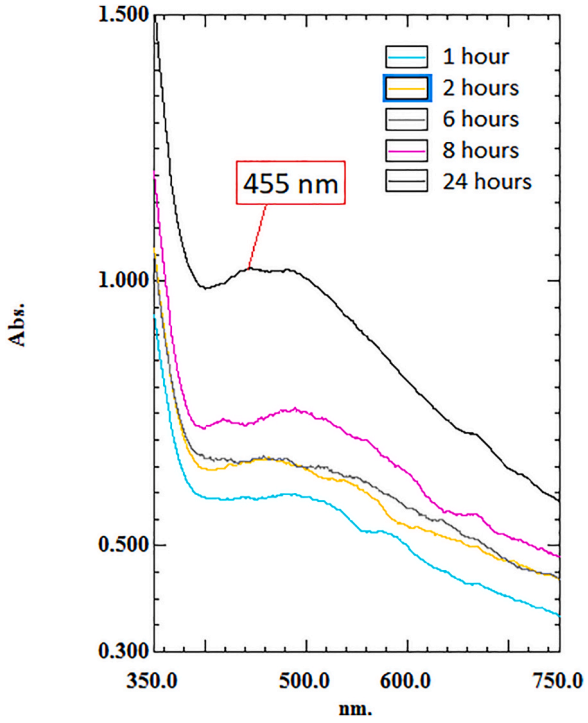

Fig. 4. UV–Vis spectra of MP-AgNPs at 1, 2, 6, 8 and 24 h. The wavelength range used between 350 and 800 nm.

interaction via hydrogen bonding between the reduced silver and stabilising agent contained in the *M. porteri* extract [8].

3.3.3. FTIR analysis

Fig. 5 shows the FTIR spectrum of *M. porteri* extract (5A) and MP-AgNPs (5B). For *M. porteri* extract spectrum, the broad absorption band observed at 3300 cm^{-1} represented the O–H stretching group of the phenolic compounds, which indicated the presence of strong hydrogen bonding [32]. The bands observed at 2957 cm^{-1}, 2920 cm^{-1} and 2853 cm^{-1} were attributed to the stretching vibration of the C–H bond in the aliphatic hydrocarbon chains [33]. The absorption band at 1601 cm^{-1} was attributed to N–H bending of amines [34].

MP-AgNPs had similar absorption bands with *M. porteri* extract at 3300 cm^{-1} which indicated the presence of O–H stretching group [32] and at 2957 cm^{-1} represented C–H stretch group [33]. The other bands of MP-AgNPs were discovered to have almost similar spectra to *M. porteri* extract with minor shifts at 2923 cm^{-1} and 2853 cm^{-1}, both indicated C–H stretch of aldehyde [35]. The

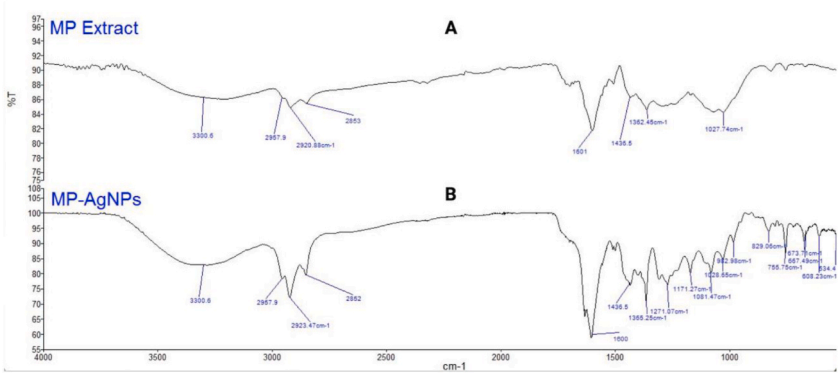

Fig. 5. FTIR Spectra of *M. porteri* extract (A) and MP-AgNPs (B).

absorption bands at 1600 cm^{-1} and 1365 cm^{-1} attributed to the N–H group of amine and C–N stretch group respectively [34].

As may be seen from the figure, both samples exhibit identical spectra. The phytochemical compounds of *M. porteri* extract still appear in the spectrum of MP-AgNPs, implying that the phytochemical compounds formed complexes with the silver and remained on the surface of the AgNPs [36]. It showed that the phytochemicals are actively participating in the reduction and stabilisation of AgNPs formation [8].

3.3.4. SEM analysis

Fig. 6 shows the image of MP-AgNPs under electron microscopy. The MP-AgNPs formed were well dispersed and round in shape. The measured size of one of the nanoparticles was 93.04 nm, indicating that the size of synthesised MP-AgNPs falls within the desired size range of nanoparticles which is 1–100 nm in diameter [5]. Even though SEM is beneficial for morphological and size analysis, it has limited application since it is unable to analyze the particle size distribution [23].

3.3.5. Particle size analysis

Particle size has a significant impact on the physicochemical properties of nanoparticles. Nanoparticles are more efficient in delivering drugs than microparticles because the small size of nanoparticles allows a greater surface area for drug interaction [23]. Fig. 7 (a) shows the result of the particle size analysis of synthesised MP-AgNPs. The average size of MP-AgNPs was 64 nm, and the average particle size was close to the size estimated by SEM. Meanwhile, the Polydispersity Index (PDI) of MP-AgNPs was 0.136. PDI below 0.5 suggests a relatively narrow particle size distribution which indicates the particles of MP-AgNPs have a similar size [37].

Fig. 6. SEM image of synthesised MP-AgNPs. The indicated size is 93.04 nm.

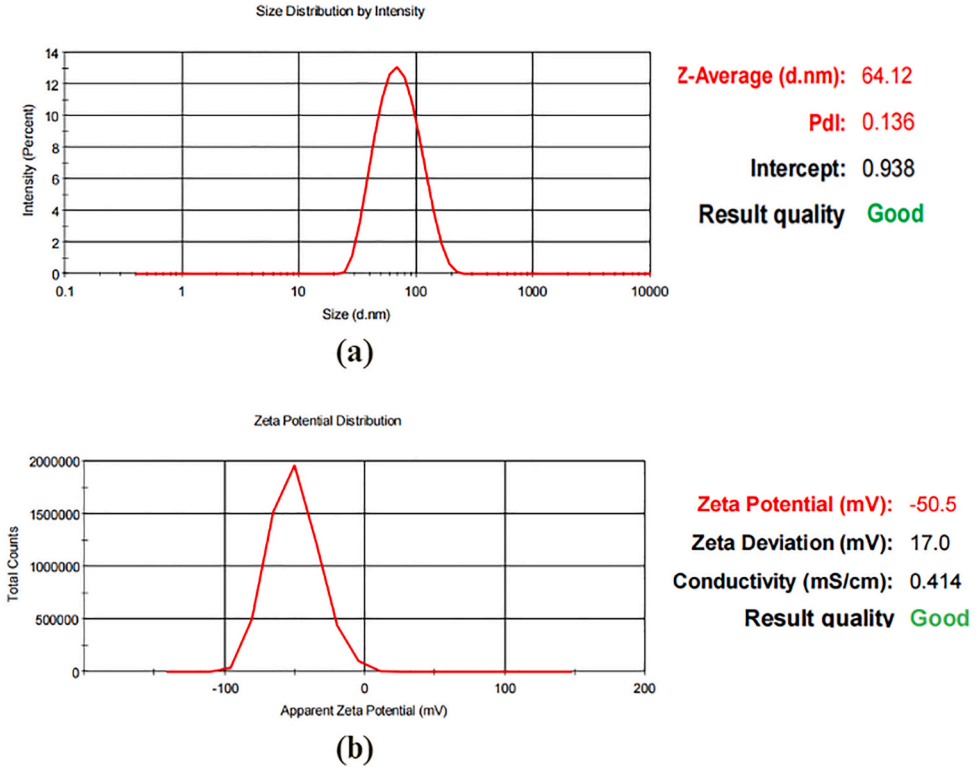

Fig. 7. (a) Size distribution of synthesised MP-AgNPs analysis using particle size analyzers. (b) Zeta potential distribution of synthesised MP-AgNPs using zetasizer.

3.3.6. Zeta potential analysis

By measuring zeta potential, it can provide information regarding the surface charges and predict the stability of the colloidal dispersion [23]. As shown in Fig. 7 (b), the zeta potential of MP-AgNPs is −50.5 mV. Nanoparticles have good stability and little nanoparticle aggregation when the zeta potential is above +30 mV or below −30 mV [4]. MP-AgNPs have a negative zeta potential, which suggests that negatively charged functional groups were responsible for the nanoparticles' stability [26].

3.4. Antibacterial study

Since AgNPs have been reported to have good antibacterial activity, the microbial activity of synthesised MP-AgNPs was evaluated against four different bacterial strains; 2 g-positive bacteria (*B. subtilis and S. aureus*), and 2 g-negative bacteria (*E. coli, and P. aeruginosa*). Disk diffusion method was employed for this assay. Fig. 8 shows zone of inhibition of MP-AgNPs, *M. porteri* extract, $AgNO_3$ and the controls.

MP-AgNPs (1.2 mg/mL) showed antibacterial activity against *B. subtilis, S. aureus, E. coli,* and *P. aeruginosa* with inhibitory zones of 8.0 ± 0.36 mm, 8.5 ± 0.45 mm, 7.5 ± 0.36 mm, and 9.0 ± 0.40 mm respectively. It cannot be concluded whether the nanoparticles have better antimicrobial activity against gram-positive or gram-negative bacteria since the zone of inhibition were almost similar. The AgNPs have the highest antibacterial activity against *P. aeruginosa* and least activity against *E. coli*. For *M. porteri* extract, it did not show any antibacterial activity against the four bacterial strains. Taher and coworkers also did an antimicrobial study of haplophytin B, one of the compounds in *M. porteri* against the four bacterial strains and the results were the same [18].

The antimicrobial activity of $AgNO_3$ was also evaluated to compare its activity with MP-AgNPs. The antimicrobial activity of MP-AgNPs, *M. porteri* extract, $AgNO_3$, and controls is presented in Table 2. In this study, there was not much difference between gram-positive and gram-negative bacterial strains in terms of the antibacterial activity of MP-AgNPs. The zone of inhibition for $AgNO_3$ against *B. subtilis, S. aureus, E. coli,* and *P. aeruginosa* were 8.0 ± 0.26 mm, 8.5 ± 0.26 mm, 8.0 ± 0.32 mm, and 10.0 ± 0.40 mm respectively. The MP-AgNPs and $AgNO_3$ had the same zone of inhibition for *B. subtilis* and *S. aureus*. However, $AgNO_3$ had better antibacterial activity against *E. coli*, and *P. aeruginosa* compared to MP-AgNPs since the zone of inhibition of $AgNO_3$ is bigger than MP-AgNPs. When compared to the controls (amoxicillin and streptomycin), MP-AgNPs and $AgNO_3$ exhibited much less antimicrobial activity.

The exact mechanism behind antibacterial activity of AgNPs is currently unknown. According to recent studies, metal nanoparticles trigger cell death in bacteria by forming long-lasting electrostatic bond with the bacterial cell walls [5]. The interaction between the positive charge of Ag^+ and the negative charge on the bacterial cell wall interferes with the structure of the cell membrane. This can

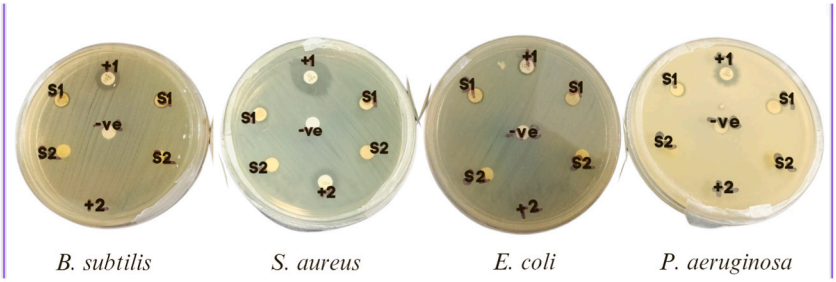

Fig. 8. Antibacterial activity of MP-AgNPs, *M. porteri* extract and $AgNO_3$ against four bacterial strains. (S1: MP-AgNPs, S2: *M. porteri* extract, -ve: Negative control (Deionised water), +1: Positive control (Amoxicillin), and +2: Positive control (Streptomycin)).

Table 2
Zone of inhibition of four different bacterial strains. The results were expressed as mean ± standard error.

Strain	Zone of Inhibition (mm)				
	MP-AgNPs	*M. Porteri* extract	$AgNO_3$	Control (Amoxicillin)	Control (Streptomycin)
B. subtilis	8.0 ± 0.36[a,b]	–	8.0 ± 0.26	9.0 ± 0.38	18.0 ± 0.36
S. aureus	8.5 ± 0.45[a,b]	–	8.5 ± 0.26	17.5 ± 0.49	17.0 ± 0.36
E. coli	7.5 ± 0.36[a,b]	–	8.0 ± 0.32	8.0 ± 0.41	16.0 ± 0.29
P. aeruginosa	9.0 ± 0.40[a,b]	–	10 ± 0.40	13.5 ± 0.45	19.0 ± 0.29

[a] = significancly different to amoxicillin control, p = 0.05.
[b] = significancly different to streptomycin control, p = 0.05.

increase cell permeability which can cause damage to the cell membrane and consequently lead to cell leakage [7]. Plus, the interaction of AgNP with DNA may impede bacterial cell division and DNA replication, resulting in cell death [38].

3.5. Cytotoxic study

MP-AgNPs did not show significant cytotoxic activity in Caco-2 and MCF-7 cells. The percentage of cell viability for both cells was above 85%. According to Alyami et al. the concentration of nanoparticles is directly proportional to the number of cell deaths. However, the result showed that the viability of Caco-2 and MCF-7 cells fluctuated at increasing concentrations of MP-AgNPs. Plus, the standard errors for Caco-2 cells and MCF-7 cells were high which indicated that the results were inaccurate and did not represent the true percentage of the cell viability [3].

It may be caused by an interference of reading by a microplate reader on colloidal silver nanoparticles dispersed in the medium. In addition, the inaccurate results from this study may be attributed to multiple factors such as low concentration of MP-AgNPs, different cell densities for each well, duration of cells incubated with MTT reagent and metabolic activity of the cells [39].

However, in many researches, green synthesised AgNPs are scientifically proven to have antiproliferative and apoptosis-inducing effects [10]. By using MTT assay, Caco-2 cells and MCF-7 cells were treated with MP-AgNPs at various concentrations; 400 μg/ml, 200 μg/ml, 100 μg/ml, 50 μg/ml, 25 μg/ml and 12.5 μg/ml in the 96-well plates.

Based on the previous study, the green synthesised AgNPs exhibited cytotoxic activity against various cancer lines such as HepG2 [3], BEAS-2B [28], MCF-7 and A549 [27]. Meanwhile, Arumai Selvan reported that the AgNPs produced by green synthesis with garlic, green tea and turmeric possessed IC_{50} of 19.94, 20.97 and 11.65 mg/mL against MCF-7, respectively [40].

The mechanisms by which AgNPs affect cancer cells are intricate and understudied. One of the proposed mechanisms is that AgNPs get into the mitochondria through endocytosis, which causes the production of ROS. AgNPs are toxic to malignant cells and can cause oxidative stress that results in DNA damage, mitochondrial damage, and induction of apoptosis [10]. The toxicity of nanoparticles may differ depending on the different cell lines. The size of the metal nanoparticles is another important element in the cytotoxic activity of cancerous cells. Smaller particles have better cytotoxic activity due to the larger surface area that can interact with the cells [29]. However, the intrinsic factors such as the physical properties of nanoparticles may cause a limitation in *in vitro* studies for the cytotoxic activity [41].

4. Conclusion

Green synthesis of AgNPs using plant extract has been used in because of its rapid and high yield of nanoparticle production. AgNPs are one of the most commercialized fabricated nanomaterials with attractive applications in biomedical (e.g. antimicrobial and cytotoxicity). In this study, AgNPs were successfully synthesised by utilising the green synthesis method. The leaf extract of *M. porteri* contains amino acids, polyphenols, steroids, terpenoids and heterocyclic compounds are possible compounds that act as reducing and stabilising agent agents. Following characterisation, the AgNPs were round in shape and the average size was 64 nm. In the

antimicrobial test, it was found that AgNPs have antimicrobial activity against *B. subtilis, S. aureus, E. coli,* and *P. aeruginosa* but they did not significantly inhibit the growth of bacteria as amoxicillin and streptomycin. Meanwhile, in cytotoxic studies, the result showed no cytotoxic activity. Since there is limited information regarding *M. porteri*, more research needs to be conducted related to M. *porteri* as a reducing agent for the synthesis of metal nanoparticles.

CRediT authorship contribution statement

Nadhirah Badrillah: Writing – original draft, Investigation. **Deny Susanti:** Supervision. **Tengku Karmila Tengku Mohd Kamil:** Supervision. **Greesty Finotory Swandiny:** Validation. **Yuli Widyastuti:** Writing – review & editing. **Erizal Zaini:** Writing – review & editing. **Muhammad Taher:** Writing – review & editing, Supervision, Conceptualization.

Declaration of competing interest

The authors declare the following financial interests/personal relationships which may be considered as potential competing interests: The authors declare no conflict of interest.

Muhammad Taher reports administrative support was provided by International Islamic University Malaysia. If there are other authors, they declare that they have no known competing financial interests or personal relationships that could have appeared to influence the work reported in this paper.

Acknowledgements

The authors would like to thank Dr. Mohd Fadly Mohd Noor from Basic Medical Science Department, Kulliyyah of Medicine, the International Islamic University Malaysia for Scanning Electron Microscopy measurement.

References

[1] Pr Shankar, Book review: tackling drug-resistant infections globally, Arch Pharma Pract 7 (2016) 110, https://doi.org/10.4103/2045-080X.186181.
[2] J. Zhou, Y. Kang, L. Chen, H. Wang, J. Liu, S. Zeng, L. Yu, The drug-resistance mechanisms of five platinum-based antitumor agents, Front. Pharmacol. 11 (2020) 343, https://doi.org/10.3389/fphar.2020.00343.
[3] N.M. Alyami, H.M. Alyami, R. Almeer, Using green biosynthesized kaempferol-coated sliver nanoparticles to inhibit cancer cells growth: an in vitro study using hepatocellular carcinoma (HepG2), Cancer Nano 13 (2022) 26, https://doi.org/10.1186/s12645-022-00132-z.
[4] D. Susanti, M.S. Haris, M. Taher, J. Khotib, Natural products-based metallic nanoparticles as antimicrobial agents, Front. Pharmacol. 13 (2022) 895616, https://doi.org/10.3389/fphar.2022.895616.
[5] D. Anbumani, K.V. Dhandapani, J. Manoharan, R. Babujanarthanam, A.K.H. Bashir, K. Muthusamy, A. Alfarhan, K. Kanimozhi, Green synthesis and antimicrobial efficacy of titanium dioxide nanoparticles using Luffa acutangula leaf extract, J. King Saud Univ. Sci. 34 (2022) 101896, https://doi.org/10.1016/j.jksus.2022.101896.
[6] B. Goyal, N. Verma, T. Kharewal, A. Gahlaut, V. Hooda, Structural effects of nanoparticles on their antibacterial activity against multi-drug resistance, Inorganic and Nano-Metal Chemistry (2022) 1–13, https://doi.org/10.1080/24701556.2021.2025103.
[7] M.P. Patil, G.-D. Kim, Eco-friendly approach for nanoparticles synthesis and mechanism behind antibacterial activity of silver and anticancer activity of gold nanoparticles, Appl. Microbiol. Biotechnol. 101 (2017) 79–92, https://doi.org/10.1007/s00253-016-8012-8.
[8] N. Ahmad, Fozia, M. Jabeen, Z.U. Haq, I. Ahmad, A. Wahab, Z.U. Islam, R. Ullah, A. Bari, M.M. Abdel-Daim, F.M. El-Demerdash, M.Y. Khan, Green fabrication of silver nanoparticles using Euphorbia serpens kunth aqueous extract, their characterization, and investigation of its in vitro antioxidative, antimicrobial, insecticidal, and cytotoxic activities, BioMed Res. Int. 2022 (2022) 1–11, https://doi.org/10.1155/2022/5562849.
[9] L. Ye, Z. Cao, X. Liu, Z. Cui, Z. Li, Y. Liang, S. Zhu, S. Wu, Noble metal-based nanomaterials as antibacterial agents, J. Alloys Compd. 904 (2022) 164091, https://doi.org/10.1016/j.jallcom.2022.164091.
[10] D.K. Poudel, P. Niraula, H. Aryal, B. Budhathoki, S. Phuyal, R. Marahatha, K. Subedi, Plant-mediated green synthesis of Ag NPs and their possible applications: a critical review, Journal of Nanotechnology 2022 (2022) 1–24, https://doi.org/10.1155/2022/2779237.
[11] O. Ahmed, N.R.S. Sibuyi, A.O. Fadaka, M.A. Madiehe, E. Maboza, M. Meyer, G. Geerts, Plant extract-synthesized silver nanoparticles for application in dental therapy, Pharmaceutics 14 (2022) 380, https://doi.org/10.3390/pharmaceutics14020380.
[12] R. Emmanuel, S. Palanisamy, S.-M. Chen, K. Chelladurai, S. Padmavathy, M. Saravanan, P. Prakash, M. Ajmal Ali, F.M.A. Al-Hemaid, Antimicrobial efficacy of green synthesized drug blended silver nanoparticles against dental caries and periodontal disease causing microorganisms, Mater. Sci. Eng. C 56 (2015) 374–379, https://doi.org/10.1016/j.msec.2015.06.033.
[13] P.V. Kumar, S.M. Jelastin Kala, K.S. Prakash, Green synthesis derived Pt-nanoparticles using Xanthium strumarium leaf extract and their biological studies, J. Environ. Chem. Eng. 7 (2019) 103146, https://doi.org/10.1016/j.jece.2019.103146.
[14] Z.-R. Mashwani, M.A. Khan, T. Khan, A. Nadhman, Applications of plant terpenoids in the synthesis of colloidal silver nanoparticles, Adv. Colloid Interface Sci. 234 (2016) 132–141, https://doi.org/10.1016/j.cis.2016.04.008.
[15] E.-Y. Ahn, H. Jin, Y. Park, Assessing the antioxidant, cytotoxic, apoptotic and wound healing properties of silver nanoparticles green-synthesized by plant extracts, Mater. Sci. Eng. C 101 (2019) 204–216, https://doi.org/10.1016/j.msec.2019.03.095.
[16] S. Mukherjee, D. Chowdhury, R. Kotcherlakota, S. Patra, V. B, M.P. Bhadra, B. Sreedhar, C.R. Patra, Potential theranostics application of bio-synthesized silver nanoparticles (4-in-1 system), Theranostics 4 (2014) 316–335, https://doi.org/10.7150/thno.7819.
[17] A.C. Paiva-Santos, A.M. Herdade, C. Guerra, D. Peixoto, M. Pereira-Silva, M. Zeinali, F. Mascarenhas-Melo, A. Paranhos, F. Veiga, Plant-mediated green synthesis of metal-based nanoparticles for dermopharmaceutical and cosmetic applications, Int. J. Pharm. 597 (2021) 120311, https://doi.org/10.1016/j.ijpharm.2021.120311.
[18] M. Taher, D. Susanti, S. Abd Hamid, K. Edueng, J.M. Jaffri, A.B. Adina, M.F. Rezali, Haplophytin B from Maclurodendron porteri, Pak. J. Pharm. Sci. 27 (2014) 179–181.
[19] J.J. Kiplimo, M.S. Islam, N.A. Koorbanally, A novel flavonoid and furoquinoline alkaloids from Vepris glomerata and their antioxidant activity, Nat. Prod. Commun. 6 (2011) 1847–1850.
[20] K.-J. Won, K.-S. Chung, Y.S. Lee, M.S. Alia, M.K. Pervez, S. Fatima, J.-H. Choi, K.-T. Lee, Haplophytin-A induces caspase-8-mediated apoptosis via the formation of death-inducing signaling complex in human promyelocytic leukemia HL-60 cells, Chem. Biol. Interact. 188 (2010) 505–511, https://doi.org/10.1016/j.cbi.2010.09.001.

[21] K.M. Alarjani, D. Huessien, R.A. Rasheed, M. Kalaiyarasi, Green synthesis of silver nanoparticles by Pisum sativum L. (pea) pod against multidrug resistant foodborne pathogens, J. King Saud Univ. Sci. 34 (2022) 101897, https://doi.org/10.1016/j.jksus.2022.101897.
[22] F.N. Eze, A.J. Tola, O.F. Nwabor, T.J. Jayeoye, *Centella asiatica* phenolic extract-mediated bio-fabrication of silver nanoparticles: characterization, reduction of industrially relevant dyes in water and antimicrobial activities against foodborne pathogens, RSC Adv. 9 (2019) 37957–37970, https://doi.org/10.1039/C9RA08618H.
[23] J.K. Patra, K.-H. Baek, Green nanobiotechnology: factors affecting synthesis and characterization techniques, J. Nanomater. (2014) 1–12, https://doi.org/10.1155/2014/417305, 2014.
[24] M. Bimakr, A. Ganjloo, S. Zarringhalami, E. Ansarian, Ultrasound-assisted extraction of bioactive compounds from Malva sylvestris leaves and its comparison with agitated bed extraction technique, Food Sci. Biotechnol. 26 (2017) 1481–1490, https://doi.org/10.1007/s10068-017-0229-5.
[25] M.S. Rosdy, M.S. Rofiee, N. Samsulrizal, M.Z. Salleh, L.K. Teh, Understanding the effects of Moringa oleifera in chronic unpredictable stressed zebrafish using metabolomics analysis, J. Ethnopharmacol. 278 (2021) 114290, https://doi.org/10.1016/j.jep.2021.114290.
[26] G. Suriyakala, S. Sathiyaraj, R. Babujanarthanam, K.M. Alarjani, D.S. Hussein, R.A. Rasheed, K. Kanimozhi, Green synthesis of gold nanoparticles using Jatropha integerrima Jacq. flower extract and their antibacterial activity, J. King Saud Univ. Sci. 34 (2022) 101830, https://doi.org/10.1016/j.jksus.2022.101830.
[27] B. Shelembe, N. Mahlangeni, R. Moodley, Biosynthesis and bioactivities of metal nanoparticles mediated by Helichrysum aureonitens, J Anal Sci Technol 13 (2022) 8, https://doi.org/10.1186/s40543-022-00316-7.
[28] M. Muhamad, N. Ab Rahim, W.A. Wan Omar, N.N.S. Nik Mohamed Kamal, Cytotoxicity and genotoxicity of biogenic silver nanoparticles in A549 and BEAS-2B cell lines, Bioinorgan. Chem. Appl. 2022 (2022) 1–22, https://doi.org/10.1155/2022/8546079.
[29] P. Kuppusamy, S.J.A. Ichwan, P.N.H. Al-Zikri, W.H. Suriyah, I. Soundharrajan, N. Govindan, G.P. Maniam, M.M. Yusoff, In Vitro anticancer activity of Au, Ag nanoparticles synthesized using Commelina nudiflora L. Aqueous extract against HCT-116 colon cancer cells, Biol. Trace Elem. Res. 173 (2016) 297–305, https://doi.org/10.1007/s12011-016-0666-7.
[30] S.J. Nadaf, N.R. Jadhav, H.S. Naikwadi, P.L. Savekar, I.D. Sapkal, M.M. Kambli, I.A. Desai, Green synthesis of gold and silver nanoparticles: updates on research, patents, and future prospects, Open 8 (2022) 100076, https://doi.org/10.1016/j.onano.2022.100076.
[31] M.M.H. Khalil, E.H. Ismail, K.Z. El-Baghdady, D. Mohamed, Green synthesis of silver nanoparticles using olive leaf extract and its antibacterial activity, Arab. J. Chem. 7 (2014) 1131–1139, https://doi.org/10.1016/j.arabjc.2013.04.007.
[32] S. Hamedi, S.A. Shojaosadati, A. Mohammadi, Evaluation of the catalytic, antibacterial and anti-biofilm activities of the Convolvulus arvensis extract functionalized silver nanoparticles, J. Photochem. Photobiol. B Biol. 167 (2017) 36–44, https://doi.org/10.1016/j.jphotobiol.2016.12.025.
[33] S.J. Jang, I.J. Yang, C.O. Tettey, K.M. Kim, H.M. Shin, In-vitro anticancer activity of green synthesized silver nanoparticles on MCF-7 human breast cancer cells, Mater. Sci. Eng. C 68 (2016) 430–435, https://doi.org/10.1016/j.msec.2016.03.101.
[34] L. Sherin, A. Sohail, U.-S. Amjad, M. Mustafa, R. Jabeen, A. Ul-Hamid, Facile green synthesis of silver nanoparticles using Terminalia bellerica kernel extract for catalytic reduction of anthropogenic water pollutants, Colloid and Interface Science Communications 37 (2020) 100276, https://doi.org/10.1016/j.colcom.2020.100276.
[35] L. Karthik, G. Kumar, A.V. Kirthi, A.A. Rahuman, K.V. Bhaskara Rao, Streptomyces sp. LK3 mediated synthesis of silver nanoparticles and its biomedical application, Bioproc. Biosyst. Eng. 37 (2014) 261–267, https://doi.org/10.1007/s00449-013-0994-3.
[36] F.A. Lubis, N.A.N.N. Malek, N.S. Sani, K. Jemon, Biogenic synthesis of silver nanoparticles using Persicaria odorata leaf extract: antibacterial, cytocompatibility, and in vitro wound healing evaluation, Particuology 70 (2022) 10–19, https://doi.org/10.1016/j.partic.2022.01.001.
[37] A. Evans, Peddie Song, A. Evans, Particle size reduction to the nanometer range: a promising approach to improve buccal absorption of poorly water-soluble drugs, IJN (2011) 1245, https://doi.org/10.2147/IJN.S19151.
[38] B. Buszewski, V. Railean-Plugaru, P. Pomastowski, K. Rafińska, M. Szultka-Mlynska, P. Golinska, M. Wypij, D. Laskowski, H. Dahm, Antimicrobial activity of biosilver nanoparticles produced by a novel Streptacidiphilus durhamensis strain, J. Microbiol. Immunol. Infect. 51 (2018) 45–54, https://doi.org/10.1016/j.jmii.2016.03.002.
[39] M. Ghasemi, T. Turnbull, S. Sebastian, I. Kempson, The MTT assay: utility, limitations, pitfalls, and interpretation in bulk and single-cell analysis, IJMS 22 (2021) 12827, https://doi.org/10.3390/ijms222312827.
[40] D. Arumai Selvan, D. Mahendiran, R. Senthil Kumar, A. Kalilur Rahiman, Garlic, green tea and turmeric extracts-mediated green synthesis of silver nanoparticles: phytochemical, antioxidant and in vitro cytotoxicity studies, J. Photochem. Photobiol. B Biol. 180 (2018) 243–252, https://doi.org/10.1016/j.jphotobiol.2018.02.014.
[41] L. Liu, Z. Zhang, L. Cao, Z. Xiong, Y. Tang, Y. Pan, Cytotoxicity of phytosynthesized silver nanoparticles: a meta-analysis by machine learning algorithms, Sustainable Chemistry and Pharmacy 21 (2021) 100425, https://doi.org/10.1016/j.scp.2021.100425.